Transition Radiation from Relativistic Electrons Crossing Dielectric Boundaries

FRED W. INMAN*
University of the Pacific, Stockton, California
AND
J. J. MURAY
Hewlett-Packard Company, Palo Alto, California
(Received 30 September 1965)

A coincidence technique has been used to observe transition radiation from fast electrons crossing the boundary between a vacuum and a dielectric. Gold, nickel, aluminum, and Mylar were the dielectrics used. A photomultiplier was used to count single photons in coincidence with the arrival of the electron at the boundary, as observed with a lithium-drifted germanium detector. The electrons were from a cesium-137 source. The relative photon yields for the three metals were: Al yield/Au yield $=1.03\pm0.22$, Ni yield/Au yield $=0.61\pm0.09$. The absolute yield for gold was $(10\pm3)\times10^{-3}$ photons per electron, in agreement with theory. The results with Mylar are complicated by fluorescence effects, but there is evidence that the transition-radiation yield is of the same order of magnitude as the yield in gold. The yield was measured as a function of electron energy; it is a monotonically increasing function of the energy from 0.33 MeV to 0.662 MeV, in qualitative agreement with theory.

INTRODUCTION

TWENTY years ago Frank and Ginsburg[1] predicted the existence of a weak radiation which should be observed as a charged particle crosses the boundary between two media of different dielectric properties. Several other authors[2–5] have discussed the problem theoretically over the intervening years, but only recently has this transition radiation been investigated experimentally. Goldsmith and Jelley[6] established the existence of this radiation for protons from a 5-MeV Van de Graaff generator. However, the transition radiation produced by relativistic particles has not previously been established.

Garibian[2] obtains the following formula for the Poynting vector flux per unit solid angle due to transition radiation for a particle passing from vacuum to a medium characterized by a complex dielectric constant $\epsilon=\epsilon_1+i\epsilon_2$:

$$\frac{dW}{d\Omega}=\frac{e^2\sin^2\theta\cos^2\theta}{\pi^2 c}\frac{\beta^2}{(1-\beta^2\cos^2\theta)^2}\times\int_0^\infty\left|\frac{(\epsilon-1)(1-\beta^2+\beta(\epsilon-\sin^2\theta)^{1/2})}{(\epsilon\cos\theta+(\epsilon-\sin^2\theta)^{1/2})(1+\beta(\epsilon-\sin^2\theta))}\right|d\omega. \quad (1)$$

In this formula θ is the angle between the direction of the incoming charged particle and the direction of the outgoing photon (see Fig. 1), β is the particle velocity, c is the velocity of light, and ω is the angular frequency of the radiation. This equation can be re-expressed in terms of the photon flux by using the fact that for photons of angular frequency ω, the energy dW, associated with dN photons is

$$dW=(\hbar\omega)dN. \quad (2)$$

The result is

$$\frac{dN}{d\Omega}=\frac{\alpha\beta^2}{\pi^2}\frac{\sin^2\theta\cos^2\theta}{(1-\beta^2\cos^2\theta)^2}\times\int_0^\infty\left|\frac{(\epsilon-1)(1-\beta^2+\beta(\epsilon-\sin^2\theta)^{1/2})}{(\epsilon\cos\theta+(\epsilon-\sin^2\theta)^{1/2})(1+\beta(\epsilon-\sin^2\theta)^{1/2})}\right|^2\frac{d\omega}{\omega}, \quad (3)$$

where α is the fine structure constant. If the dielectric constant is known as a function of frequency over the range of interest, then the integral of Eq. (3) can be numerically evaluated.

Furthermore, Garibian shows that the transition is plane polarized in the plane of Fig. 1.

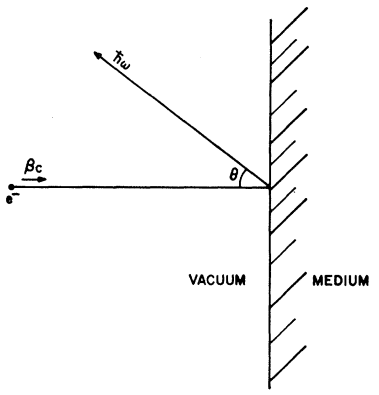

FIG. 1. Geometry illustrating production of transition radiation.

* This work was carried out while this author was a guest of the Nuclear Physics group of the Hewlett-Packard Company.

[1] I. M. Frank and V. L. Ginzburg, Zh. Eksperim. i Teor. Fiz. **16**, 15 (1945); J. Phys. USSR **9**, 353 (1945).
[2] G. M. Garibian, Zh. Eksperim. i Teor. Fiz. **33**, 1403 (1957) [English transl.: Soviet Phys.—JETP **6**, 1079 (1958)].
[3] G. Beck, Phys. Rev. **74**, 795 (1948).
[4] N. P. Klepicov, Vestn. Mosk. Univ. **8**, 6 (1951).
[5] N. A. Korkhazian, Izv. Akad. Nauk Arm. SSR Ser. Fiz. Mat. Nauk **10**, 4 (1957).
[6] P. Goldsmith and J. V. Jelley, Phil. Mag. **4**, 836 (1959).

EXPERIMENT DESIGN

The feasibility of this experiment rests upon the possibility of observing single photon pulses in coincidence with the arrival of single charged particles at the boundary between the vacuum and the medium. This was accomplished by using an RCA 8575 photomultiplier to observe the single photons and a lithium-drifted silicon detector to observe the 0.662-MeV internal-conversion electrons from a thin 50-μc: cesium-137 source. This arrangement of the photomultiplier, detector, and source, within a vacuum chamber, is sketched in Fig. 2. The transmission of the quartz window in Fig. 2 is essentially 100% throughout the spectral range of the photomultiplier. The type HNP[1]B polaroid was chosen to optimize the transmission of photons throughout the spectral range of the photomultiplier. The vacuum of about 8μ was obtained from a mechanical pump.

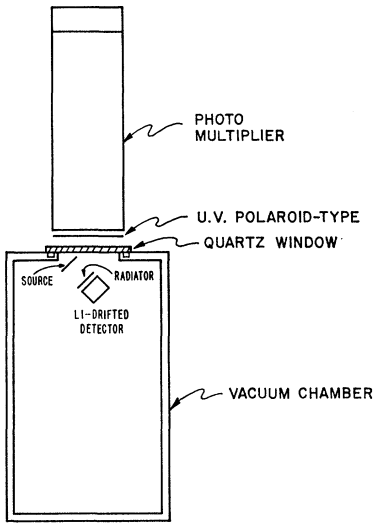

FIG. 2. Arrangement of the apparatus.

The radiator used in Fig. 2 was either a thin foil or the semiconductor detector itself, which is coated with approximately 200 Å of gold. The foils used were sufficiently thin that there was no significant reduction in pulse size at the solid-state detector due to energy loss in the foils.

A block diagram of the electronics is shown in Fig. 3. The photomultiplier pulse, which has a rise time of about 4 nsec, is amplified by a fast amplifier and goes to a fast discriminator. The discriminator level is set to correspond to the threshold for single photon events. Figure 4 shows two pulse-height spectra, one with the photocathode dark and the other with a very weak illumination of the photocathode. It is clear from this figure where the discriminator should be set. The standard pulse output of the discriminator can be switch selected for a width of approximately 40 nsec, as measured on an oscilloscope. A second discriminator is triggered by the output pulse of the first discriminator

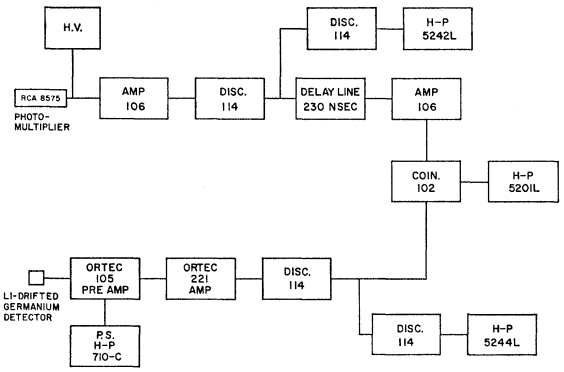

FIG. 3. Block diagram of electronics. Numbers refer to Chronetics model numbers.

and provides a wide pulse (approximately 160 nsec) required by the 5242L counter. A delay cable is needed in the photomultiplier side of the coincidence circuit to compensate for amplifier delays in the solid-state side of the coincidence circuit. The exact amount of delay was determined experimentally by adjusting cable length for maximum coincidence rate, keeping singles rates constant.

The solid-state detector was operated at a bias of 200 V, which provides ample depletion depth to stop the internal-conversion electrons. The solid-state pulses are

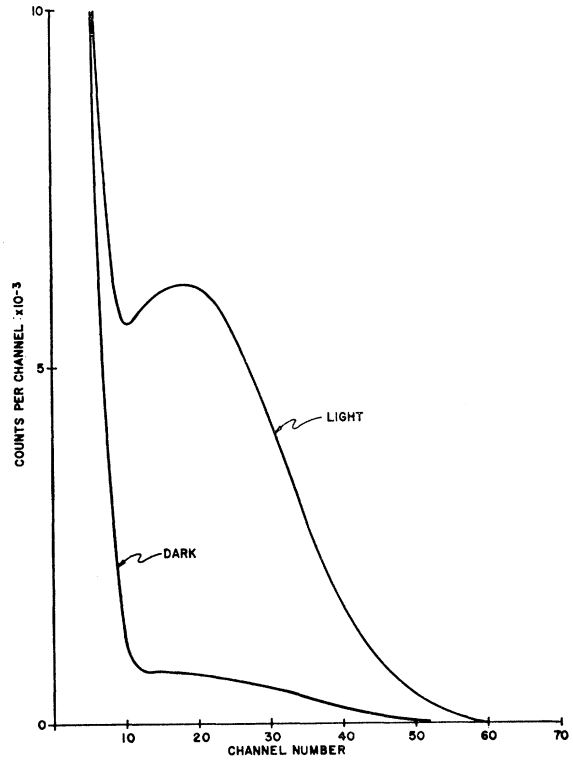

FIG. 4. Pulse-height spectra of RCA 8575 photomultiplier at a high voltage of 1600 V for dark cathode and for very weakly illuminated cathode. A Nuclear Data ND-180*F* analyzer was used.

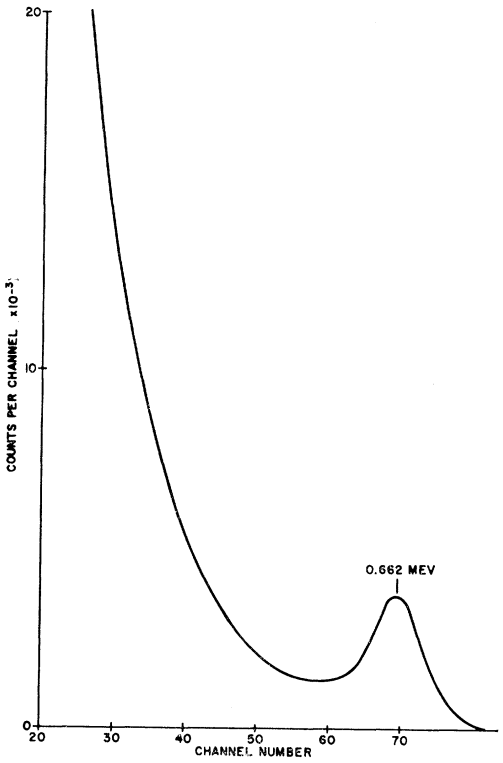

FIG. 5. Beta-spectrum of CS-137 taken on Nuclear Data ND-180 analyzer. The pulses were doubly differentiated with $RC=0.1$ μsec.

integrated in the charge-sensitive preamplifier and doubly RC differentiated in the Ortec 221 main amplifier. The time constants for both differentiations were 0.1 μsec. The use of such a short time constant results in the degradation of pulse-height resolution, but it is necessary in order to take advantage of the comparatively fast coincidence circuit to be used. The pulse-height spectrum for the solid-state detector, using the short time-constant differentiation, is shown in Fig. 5. The first discriminator has an output pulse width of approximately 40 nsec and drives both the coincidence circuit and a second discriminator which provides a wider pulse for the 5244L counter. The output of the coincidence circuit is counted on the 5201L counter.

The photomultiplier counting rate was approximately 10^3 times as great as the coincidence counting rate. Furthermore, the photomultiplier rate was almost completely independent of polarizer angle. On the other hand, the coincidence counting rate was dependent upon the polarizer angle and corresponded to a linear polarization of virtually 100%. According to theory the coincidence rate as a function of the polarizer angle, solid state counting rate N_s, and photomultiplier counting rate N_p, is

$$C=2\tau N_s N_p+\delta N_s \cos^2\theta. \quad (4)$$

In this equation 2τ is the resolution of the coincidence circuit and $\delta \cos^2\theta$ is the fraction of the solid-state counts that gives rise to a detected photon. Dividing Eq. (4) by $(N_s N_p)$ yields

$$C/N_s N_p=2\tau+\delta \cos^2\theta/N_p, \quad (5)$$

which is a function of the form

$$R(\theta)=a+b \cos^2\theta. \quad (6)$$

The measured discriminator output pulse width of 40 ± 4 nsec makes the first term of Eq. (5) approximately 80 nsec.

Figure 6 shows the experimental values of $C/(N_s N_p)$ versus polarizer angle and a least squares fit of Eq. (6). A polarizer angle of 0° corresponds to transmission of a photon polarized in the plane of Fig. 1. The good $\cos^2\theta$ fit is evidence that the nonaccidental component of the coincidence counting rate, which is presented by the second term on the right side of Eq. (5) is virtually completely plane polarized in the plane of Fig. 1.

The numerical integration of Eq. (3) was carried out on a Burroughs 5500 computer taking gold as the medium on which the transition radiation is produced. Although the gold film on the solid-state detector is

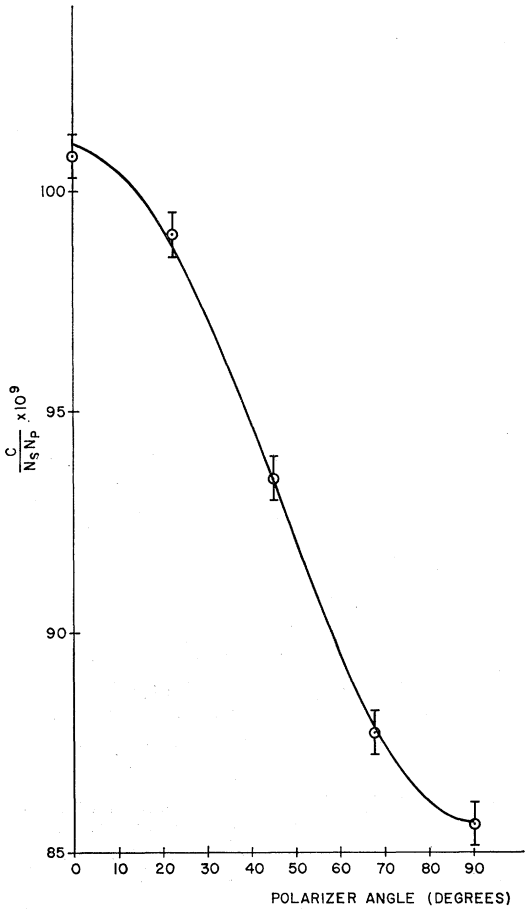

FIG. 6. Least-squares fit of $a+b \cos 2\theta$ to experimental values of $C/N_s N_p$ versus polarizer angle.

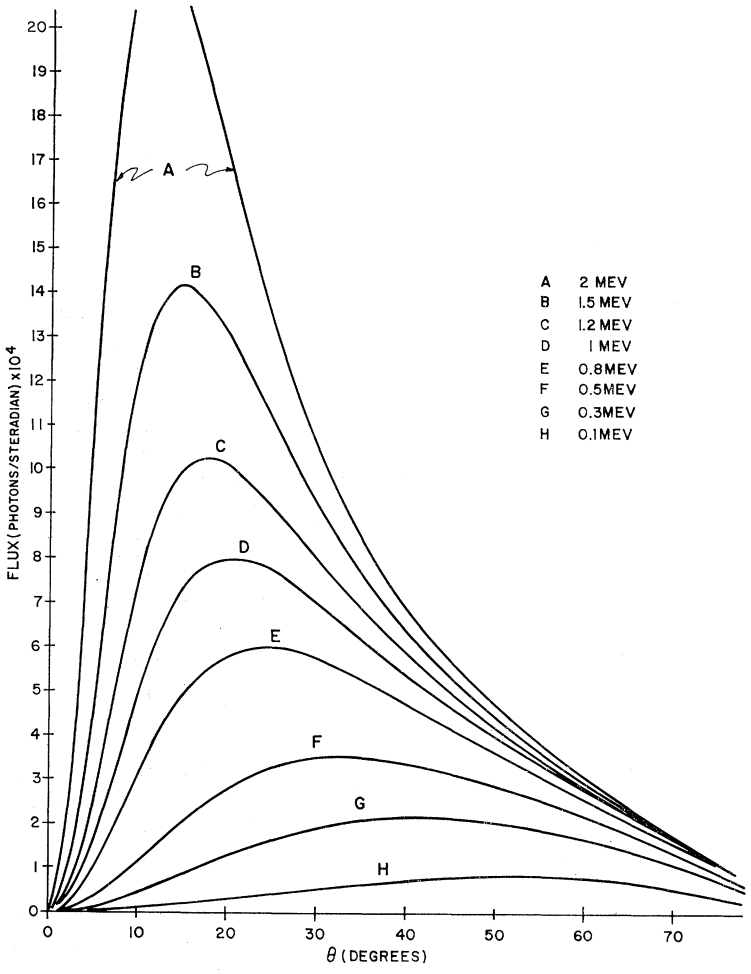

FIG. 7. Calculated flux of transition radiation from gold as a function of electron energy and production angle.

only about 200 Å thick there is evidence[7] that this thickness is sufficient to justify using the dielectric properties of bulk gold. We used the data of Phillip[7] and extrapolated it through the spectral region of the photomultiplier.

The quantum efficiency of the photomultiplier and the transmission of the polaroid are functions of wavelength and must be considered in the numerical integration of Eq. (3). The quantum efficiency was obtained from the manufacturer's specification sheet, and the transmission of the polaroid was measured on a spectrophotometer.

Figure 7 was plotted from the numerical integration of Eq. (3) over the wavelength range from 2500 to 6000 Å, taking the transmission of the polaroid and the quantum efficiency of the photomultiplier to be 100% to illustrate the magnitude of the effect, irrespective of photomultiplier and polaroid properties. This gives an estimated photon flux of approximately 3×10^{-4} photons per steradian per electron at 0.5 MeV. This is indeed a small effect, and the nonideal properties of the polaroid and photomultiplier cause the observed effect to be smaller than this ideal value by a factor of about 16.

RESULTS

Runs were made using various thin films, as well as the bare surface of the solid-state detector itself, as the radiator. Nickel, gold, aluminum, and Mylar foils were used. The results for the metals were substantially the same. Ratios of photon yield per electron are listed in Table I for the sake of comparison. In the table, SS stands for the photon yield from the bare solid-state detector.

The second entry in the table indicates that the transition radiation occurs within a fraction of a wavelength of the surface of the metal. This is not surprising considering Philip's measurements which show that the dielectric constant for gold as a function of film thickness is essentially constant for thicknesses greater than 0.02 μ. Transition radiation is expected to be produced in a region of changing dielectric constant, and this change occurs in a fraction of a wavelength.

A calculation[8] of the optical bremsstrahlung which is

[7] R. Philip, Compt. Rend. **247**, 1104 (1958).

[8] R. H. Ritchie, J. C. Ashley, and L. C. Emerson, Phys. Rev. **135**, A759 (1964).

TABLE I. Photon yield per electron for various radiators. SS = solid-state detector.

Radiators	Yield Ratio
1-μ Al foil / 0.001-in. Al foil	1.33±0.30
0.1-μ gold foil / SS	1.08±0.24
0.001-in. Al foil / SS	1.03±0.22
Nickel foil / SS	0.61±0.09

associated with transition radiation shows that the bremsstrahlung component is proportional to the rms multiple scattering angle of the particle as it moves through the medium. However, bremsstrahlung photons produced at depths greater than the penetration depth for optical photons do not escape from the medium, and the rms scattering within the transparent region of the metal is on the order of 10^{-3} for Ag and even smaller [because of the $Z(Z+1)$ dependence of scattering] in Al.

The factor which multiplies the rms multiple-scattering angle is a complicated function of the dielectric properties of the medium, but it is roughly the same order of magnitude as the transition radiation term. Therefore the bremsstrahlung radiation term is smaller than the transition radiation term by a factor of around 10^3. Furthermore, the bremsstrahlung radiation is generally only partially polarized. The third and fourth entries in Table I indicate that the observed radiation is comparable in Ag, Al, and Ni, which is hard to understand on the basis of bremsstrahlung alone; and furthermore, the substantial polarization in the plane expected for transition radiation makes it unlikely that the radiation observed is bremsstrahlung.

One run was made with yellow Mylar tape over the solid-state detector. This gave a coincidence rate higher than the metal foil rates by a factor of about 2.2. This higher rate corresponded to an unpolarized component of about 3×10^{-3} detected photons per solid-state count. There was also a polarized component amounting to about 5×10^{-4} detected photons per solid-state count. Accidental coincidences have been subtracted from both these figures. Undoubtedly much of the unpolarized component comes from fluorescence within the Mylar, but at least part of the polarized component is probably transition radiation, because it is difficult to imagine mechanisms by which the fluorescence radiation could be significantly polarized. The polarized component of the flux produced on Mylar is greater than the flux with the bare solid-state detector by a factor of about 2.5. It would be interesting to investigate nonmetals further, but the metals yielded more ideal results from the standpoint that the polarization was very nearly 100% for those photons corresponding to the nonaccidental coincidence counts.

TABLE II. Photon yield for four different *average* electron energies. The yield at the internal-conversion energy of 0.662 MeV is arbitrarily taken to be 1.

Average energy (MeV)	Relative photon yield
0.662	1
0.6	0.61±0.13
0.5	0.48±0.12
0.33	0.25±0.07

At relativistic energies the photon yield as a function of energy is not easily obtained from the theoretical formulas. At nonrelativistic energies, the yield is proportional to energy. At relativistic energies we may expect the yield to be a monotonically increasing function of energy, as evidenced by Fig. 7. Table II shows the results of a measurement of the photon yield for different *average* electron energies. The solid-state pulse-discriminator level was set at four different values, corresponding to four different average electron energies. The yield at the internal-conversion energy of 0.662 MeV is arbitrarily taken to be 1. This is in qualitative agreement with Fig. 7. It must be remembered that the pulse-height resolution of the solid state pulses is less than optimum because of the short resolving time used, and for this reason, the average energies, as estimated using Fig. 5, may be in error.

The integration of Eq. (3) over the hemisphere outside the metal gives the total photon yield per incident electron. For an energy of 0.662 MeV the integral over solid angle is approximately 1.4×10^{-3} photons per electron. This can be compared with the experimental result, based on 5 runs, which is $(10\pm3)\times10^{-3}$ photons per electron. The error quoted is due both to counting statistics and to estimated uncertainties in the geometry. The experimental yield is somewhat higher than would be expected from Eq. (3), but the integral over angular frequency in Eq. (3) is suspect because of the lack of data on the index of refraction of gold throughout the entire spectral range of the photomultiplier. According to Beck,[3] however, it should be possible to obtain approximately one photon per 100 electrons for electrons with velocity near c/n, where n is the index of refraction of the medium. In any case, the absolute yield is consistent with the theory.

ACKNOWLEDGMENTS

The authors would like to thank Tracy Storer, head of the Nuclear Instrumentation Section of the Hewlett-Packard Company. Thanks are also due to Tom R. Miller for his assistance. One of the authors (J.J.M.) is grateful to Professor G. Marx of Stanford University for many valuable discussions.